J. Fluid Mech. (2010), *vol.* 645, *pp.* 1–25.
doi:10.1017/S0022112009994186

BATCHELOR PRIZE LECTURE

Interfaces: in fluid mechanics and across disciplines

HOWARD A. STONE†

School of Engineering and Applied Sciences, Harvard University, Cambridge, MA 02138, USA

(Received 30 September 2009; revised 30 September 2009; accepted 18 December 2009)

The dynamics of fluid–fluid interfaces are important in diverse problems that span many disciplines in science and engineering. A series of snapshots is used to illustrate the breadth of applications that can occur in viscous low-Reynolds-number flows and I highlight theoretical and modelling ideas that are broadly useful for these, as well as other, problems. By way of illustration of unifying quantitative ideas we discuss briefly (i) the use of the Reciprocal Theorem in low-Reynolds-number flows, (ii) the use of the lubrication approximation for characterizing thin-film coating flows sometimes referred to as Landau–Levich–Derjaguin–Bretherton problems and (iii) nearly two-dimensional viscously dominated flows.

1. Introduction

When asked to summarize a subset of research contributions, it is common to struggle with the format. For this paper I chose the theme of 'interfaces', in large part because the dynamics of fluid–fluid interfaces are rich with basic questions and phenomena. In addition, the theme of interfaces emphasizes the idea that the concepts and principles of fluid dynamics frequently occur across the traditional science and engineering disciplines. Thus, in this paper various concepts are discussed and illustrated with the hope that they provide a way to link ideas and questions, both qualitative and quantitative, in a manner that emphasizes the bigger picture of fluid dynamics as a framework for unifying some physical phenomena. The selection is oriented towards viscously dominated flows.

Since the earliest days of fluid dynamics, the basic concepts have been used to bring insight to scientific questions in different disciplines. The better established ideas have helped to inform medical practice, e.g. understanding blood flow and circulation, and industrial practice and innovation, e.g. design of airplanes, coating flows and all manners of materials processing. These applications often raised new kinds of fluid dynamical questions. In many cases it was the first time fluid dynamicists were exposed to the existing practice that the research side of the questions were addressed, often building on empirical ideas derived from experience. For several views of this exchange between fundamental fluid dynamics research and applications see special papers written by J. C. R. Hunt and J. R. A. Pearson in volume 106 of *JFM* as

† Present address: Department of Mechanical & Aerospace Engineering, Princeton University, Princeton, NJ 08544, USA. Email address for correspondence: hastone@princeton.edu

part of the 25th anniversary of the Journal (Hunt 1981; Pearson 1981). Not counting self-citations, these papers have only been cited four and two times, respectively, which bode poorly for the future readership of this paper.

1.1. *A fascination with fluid dynamics*

Fluid dynamics has an intrinsic beauty that even non-scientists identify. For example, as several of my non-technical colleagues remind me when they learn that some of my research involves bubbles and drops, television commercials frequently show splashing drops or jets of liquid rising from a fluid bath following impact of an object on the surface. We all enjoy looking at phenomena that are essentially fluid dynamical, whether they are cascading sheets of water in parks and public buildings, birds hovering in the breeze, airplanes at take-off and landing, tears or legs in a glass of wine or strong liquor, the wake structure that trails ducks swimming in a lake, etc. Of course, the scientist may observe these same phenomena and think about the underlying physics and mathematics: what is the shape of the fluid stream or flow? How does the shape change in time? Is surface tension important? Is the response self-similar? Or a travelling wave? etc. We celebrate this visual beauty with the Gallery of Fluid Motion at the annual meeting of the Division of Fluid Dynamics of the American Physical Society (see e.g. van Dyke 1982; Samimy *et al.* 2004). So, it is easy to find inspiration and I am continually amazed by new research I see when visiting other labs, in talks at conferences, and that are shared with me by my group and collaborators.

The average reader of *JFM* certainly has a fascination with fluid dynamics. Perhaps the most important element of this fascination is that the basic principles we introduce have an enormous variety of applications, surprises and fascinating phenomena, and are relevant to many societally important issues (see e.g. Peregrine 1981; Biesheuvel & van Heijst 1998). Nevertheless, although we introduce fluid dynamics to students by way of a core course in a traditional discipline (engineering, mathematics, physics and earth and planetary sciences), we generally do not communicate well its intellectual beauty to the students or to our colleagues in other disciplines. The latter may be only dimly aware of the subject of fluid dynamics. Even when they are, their view may be of a mathematically oriented subject, which was well established hundreds of years ago (see e.g. some of the commentary in the 25th anniversary issue of *JFM*, volume 106). Thus, we can seek to identify opportunities to share the fascination and understanding of our fields with others, both in research collaborations and in educational forums.

1.2. *Intersections of fluid dynamics and other themes*

The basic principles in fluid dynamics, and many other classical science and engineering disciplines, are viewed as mature. On the other hand, when fluid dynamics intersects with other fields, some traditional and some evolving rapidly, then we discover new challenges and new research directions that may require new developments including analytical, numerical and experimental tools. I believe it is this kind of synergy that is the greatest source of new challenges not only for our field, but in science and engineering more generally, and that when solved can be of service to society.

The relevance of fluid dynamics to other fields has been recognized since the earliest days, e.g. Poiseuille was motivated by physiological questions. Early applications generated important research areas that are now considered subfields of fluid dynamics: e.g. acoustics (see Crighton 1981), water waves and wave phenomena more generally. Today we recognize, to name just a few, biofluid dynamics, compressible flows and gasdynamics, colloidal hydrodynamics, electrohydrodynamics,

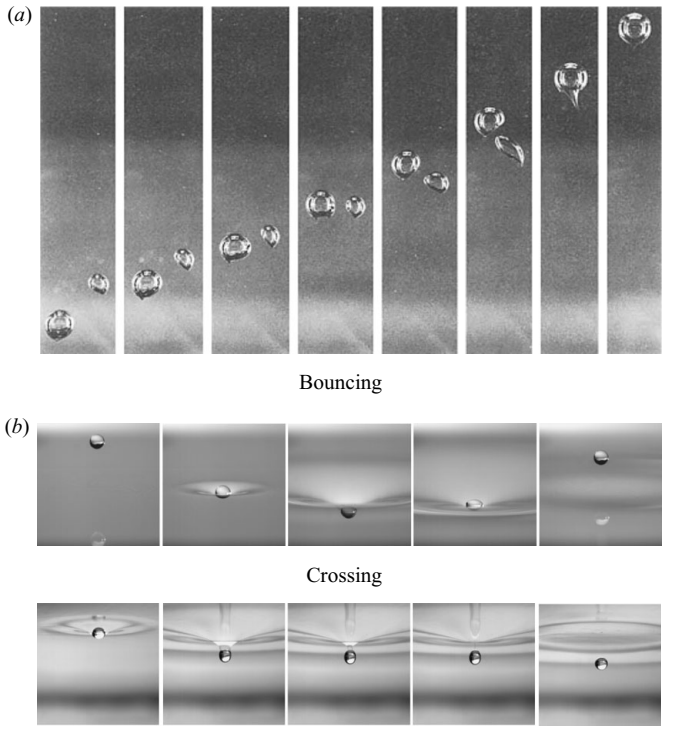

FIGURE 1. Examples of interfaces in dictating dynamics of fluid motions. (*a*) Interaction of two bubbles rising in a viscous fluid (Manga & Stone 1993). (*b*) (top) Impact of droplets on a soap film including bouncing and (bottom) passing through the film without rupture of the film (Courbin & Stone 2006).

environmental fluid dynamics, free-surface flows, geophysical fluid dynamics, ... Not surprisingly, readers will recognize subthemes that interrelate some of these topics! George Batchelor coined the term *microhydrodynamics* to highlight general themes and principles applicable to low-Reynolds-number hydrodynamics (Batchelor 1977). Although it is easy to proliferate these intersections, the main point is to recognize that they exist and common ideas can be used as building blocks when working between areas.

1.3. *Some examples of the impact of interfaces on fluid flows*

In this paper, I chose to focus on flow problems where fluid–fluid interfaces are important. For reasons of space, however, most topics are only sketched. There are an enormous variety of such problems and we discuss only low-Reynolds-number flows. Hopefully, some of the breadth and richness of fluid dynamics will be evident from the examples chosen.

To begin with, I highlight examples that show the variety of flows impacted by dynamics associated with fluid–fluid interfaces.

Consider a gas bubble or buoyant droplet rising through an immiscible fluid. At low Reynolds numbers, a spherical shape (radius a) is stable and the rise speed varies with the square of the particle radius. When two bubbles rise through the liquid their separation distance remains constant provided the bubbles are spherical, though there is a horizontal component to the rise velocity as a result of hydrodynamic interactions. As illustrated in figure 1(*a*) the hydrodynamic interactions also produce shape changes

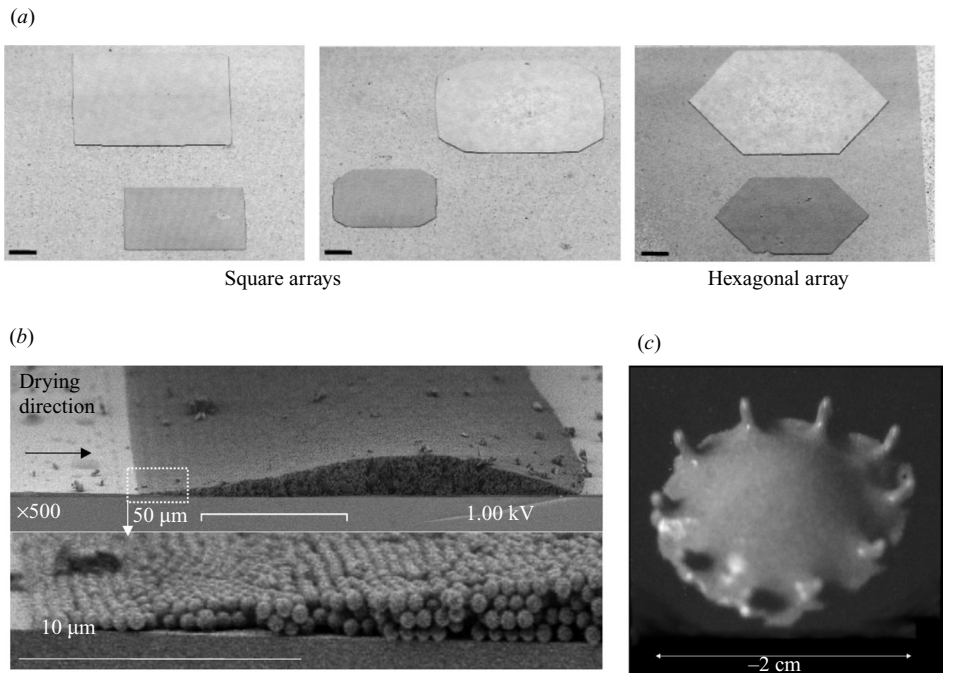

FIGURE 2. Examples of interfaces impacting dynamics on substrates. (*a*) Polygonal spreading of partially wetting liquids on microtextured surfaces (Courbin *et al.* 2007); scale bar is 1 mm. (*b*) Organization of 500 nm diameter particles at a contact line during evaporation processes (Abkarian, Nunes & Stone 2004). (*c*) A 2 cm diameter droplet of wet granular material on a vertically vibrating plate (vibration frequency equals 40 Hz) exhibits a crown-like series of oscillons (Schleier-Smith & Stone 2001).

whose magnitude depends on the Bond number, $\mathscr{B} = \Delta\rho g a^2/\gamma$, where $\Delta\rho$ is the density difference, g is the gravitational acceleration and γ is the interfacial tension. The shape changes are responsible for a significant contribution to the rise velocities of the two bubbles (or drops) that produces contact and coalescence. Figure 1(*a*) displays a dramatic example of the shape-induced interactions that occur even after the more buoyant large gas bubble passes by the vicinity of a small bubble (Manga & Stone 1993): coalescence can occur even when the two bubbles are initially well separated.

A second example involving interfaces concerns soap films, which are familiar to everyone. One aspect of these interfaces that is less well studied concerns their response to impacts such as can occur when a liquid drop is dropped on the film (see figure 1*b*): at low speeds the drop can bounce, and the subsequent dynamics can be chaotic (Gilet & Bush 2009), while at higher speeds the drop can pass through the film without breaking it. High-speed imaging illustrates that this latter feature occurs without a hole ever forming; rather the interface wraps around the drop and coalesces at the back to maintain a closed film (Courbin & Stone 2006; Le Goff *et al.* 2008).

Another example of interface dynamics is the wetting of liquids on substrates. We are all familiar with this kind of flow from pouring syrup over pancakes at breakfast. However, when the substrate contains a homogeneous microtexture, such as a square array of posts, with diameters and heights that are tens of microns, and spaced apart a comparable distance, the footprint for a partially wetting liquid can be polygonal, as exhibited in figure 2(*a*) (Courbin *et al.* 2007). In these cases, and unlike the kind of chemical patterning that can produce similar shapes due to pinned contact lines,

the polygonal drop shapes on microtextured surfaces are independent of the volume of liquid deposited, as shown in figure 2(*a*).

A fourth example involves fluids containing suspended particles. When a solvent evaporates the particles are concentrated. Often this increase in concentration is most evident at contact lines, and gives rise to the familiar coffee stain effect (Deegan *et al.* 1997). In fact, in many cases the geometric constraint provided by the wedge-shaped contact line region, along with the evaporating flow that continually supplies particles to the region of the contact line, leads to near perfect ordering of the solid phase (see figure 2*b*). In this way we can arrange nanometre-sized particles into regular patterns covering hundreds of microns if not more (Abkarian, Nunes & Stone 2004).

Other examples are not so easily characterized. For example, when a slightly wet mass of granular material is vibrated on a flat plate, the dynamics are somewhat between those for a dry granular bed, which exhibits isolated periodic eruptions or oscillons (Clément *et al.* 1996; Umbanhowar, Melo & Swinney 1996), and those of a liquid drop, where interfacial tension limits the degree of surface deformations. Figure 2(*c*) illustrates a snapshot of a phenomenon occurring at 40 Hz on a vertically vibrated plate, whereby a crown of eruptions occurs around the rim of a paste-like droplet of wet granular material (Schleier-Smith & Stone 2001). I am not aware of any explanation or calculation for the 'ring of oscillons' shown in the figure.

In recent years the subject of microfluidics has revealed many opportunities to science and engineering, by bringing new tools, allowing new ways to manipulate materials and by raising new research questions. One such avenue focuses on controlling multiphase flows. For example, a 'flow-focusing' geometry can be used for liquid–liquid (figure 3*a*) and gas–liquid (figure 3*b*) systems. Alternative geometries, such as T-junctions (figure 3*c*), have been studied. In each case, it is of interest to understand how the geometry and flow conditions set the droplet size. In these situations, numerical solutions, such as the three-dimensional simulation shown in figure 3(*d*), can be helpful for understanding the dynamics that lead to drop breakup in the confined space of the microchannel.

A further illustration of the applications of fluid mechanics is in biology. I have been fortunate to have had the opportunity to work on different problems of this type and it is an area that seems to be continually expanding. For example, in my group we have studied the deformation of individual cells in microfluidic constrictions with size comparable to that of the cell (figure 4*a*) and introduced a method to determine the change of pressure that accompanies these flows even for a single cell (Abkarian, Faivre & Stone 2006). The deformability of the cell plays an important role in haemodynamics, e.g. the Fahraeus–Lindqvist effect. We have studied one aspect of these dynamics where the drift of cells across streamlines is increasing with the shear rate, which can be used as a passive route to separate blood cells from the plasma, as shown via the contraction flow in figure 4(*b*). Throughout biology the theme of mechanotransduction is present, and mechanical stresses can produce chemical responses. Using the geometry of figure 4(*b*) we have studied the release of ATP from red blood cells (Wan, Ristenpart & Stone 2008).

As a final example, many readers will have seen movies of swimming micro-organisms, either sperm cells that propel themselves by propagating a wave along a flexible flagella, or bacterial cells, such as *E. coli*, that propel themselves using rotation of a rigid helical flagella. Most commonly the propulsion occurs in a straight line. However, when *E. coli* swims near a rigid boundary, such as a microscope slide, they have circular trajectories as a result of hydrodynamic interactions with the wall, as illustrated in figure 4(*c*, *d*) (Berg & Turner 1990; Lauga *et al.* 2005).

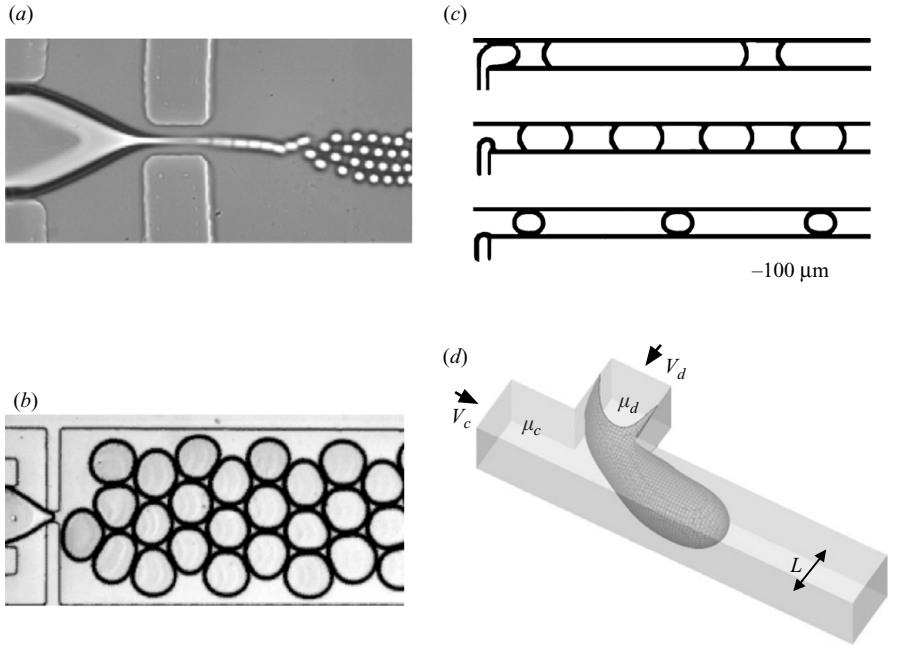

FIGURE 3. Multiphase flows in microfluidic devices. (*a*) Flow-focusing of a water-in-oil system to produce a jet that breaks into monodisperse drops. The width of the narrow orifice is 43.5 microns (Anna, Bontoux & Stone 2003). (*b*) Gas bubbles formed in water in a flow-focusing arrangement. The width of the outlet channel is 750 μm. (*c*) Nitrogen bubbles formed in surfactant-free water at a T-junction whose width is 100 microns (Garstecki *et al.* 2006). (*d*) Three-dimensional numerical simulation of drop breakup at a T-junction with square cross-section. The viscosity of the droplet phase is equal to viscosity of the continuous phase (De Menech *et al.* 2007).

A glance at the recent literature will provide many examples of how ideas generated from other areas of science and engineering continue to invigorate fluid mechanics with new directions for theory, modelling and experiments. In parallel, the principles familiar from fluid dynamics help to advance those areas. It is exciting to be able to share in these activities with colleagues around the world.

1.4. *Lessons learned: the Reciprocal Theorem, thin-film flows and nearly two-dimensional Stokes flows*

All of us develop strategies for problem solving. Over the years I have found several theoretical approaches have recurred so often in my own work that I invariably think about these ideas first when exposed to a new problem. The ideas have in common that they yield quantitative estimates and tend to bypass many details of the actual flows. In each case I think the ideas should be more widely appreciated than I sense they are. Hence, in the rest of this paper I briefly discuss, usually with an example or two, three ideas:

(i) the Reciprocal Theorem, as it is used in low-Reynolds-number hydrodynamics; this often yields answers for integrated quantities such as forces and torques without requiring the calculation of detailed velocity fields,

(ii) lubrication approaches to thin-film flows; these are useful for identifying scaling arguments for the film thickness as a function of the physical variables and

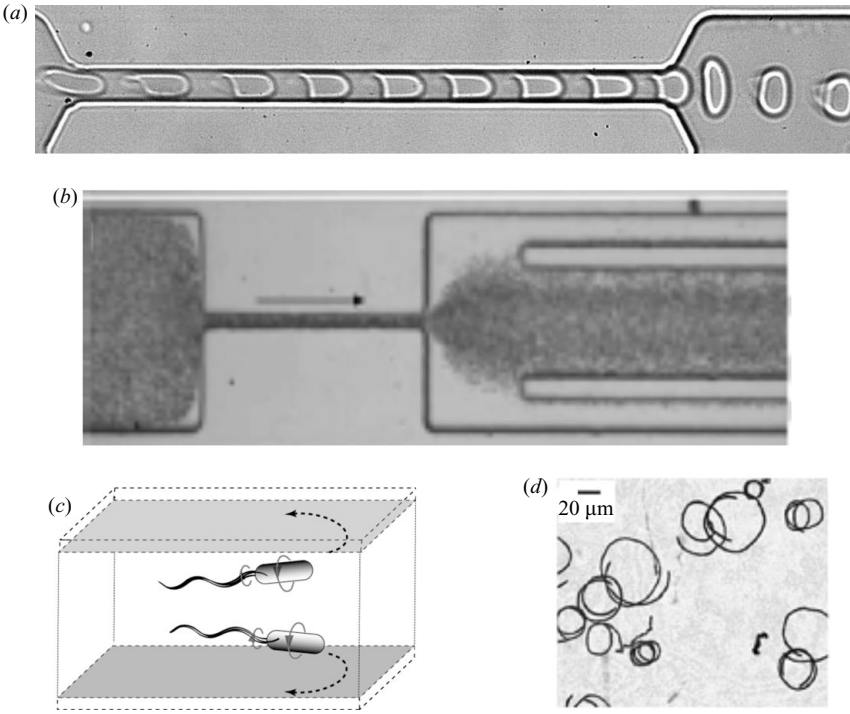

FIGURE 4. Some examples of fluid dynamics and cellular-scale biology. (*a*) Time lapse image of a red blood cell flowing through a microchannel of comparable dimensions (e.g. Abkarian, Faivre & Stone 2006). (*b*) When a suspension of cells flows through a constrictions, the cells tend to drift across streamlines and away from the wall, thus concentrating towards the centre of the channel (Faivre *et al.* 2006). (*c*) Schematic of swimming cells that turn to the right when swimming nearly parallel to a plane (viewed from the cell looking towards the plane). (*d*) Time lapse image showing the trajectories of cells that swim in circles (Lauga *et al.* 2005).

(iii) nearly two-dimensional Stokes flows; these frequently yield answers whose important characteristic is the appearance of a logarithmic term that involves the ratio of a geometric length scale to a distinct, problem-specific length scale, beyond which the flow is effectively three-dimensional (or at least a new physical effect enters).

Perhaps the reader will find the short summaries below helpful or a spring board for further reading. Throughout I have tried to emphasize the interplay of physical and mathematical arguments. In this spirit I am often reminded of a short story involving George Keith Batchelor (GKB) which is given in the postscript of a paper, in volume 212 of *JFM*, that is dedicated to Professor Batchelor on the occasion of his 70th birthday (Acrivos, Jeffrey & Saville 1990): '... the interplay between physical and mathematical arguments discussed in this paper brings to the mind of one of us (D. J. Jeffrey) an exchange that took place during a seminar in Cambridge in the mid 1970s.

SPEAKER (justifying elaborate mathematical argument): The trouble with a physical argument is that you may not get all the terms.

GKB: No, that is the trouble with a *bad* physical argument.

SEVERAL VOICES: How do you tell a good physical argument from a bad one?

GKB: That's easy: you *think*.'

2. The Reciprocal Theorem: getting something for nothing

One generally little known, or little appreciated, but useful tool in low-Reynolds-number hydrodynamics is the Reciprocal Theorem (e.g. Happel & Brenner 1983; Leal 2007). For a given geometry, this theoretical idea relates integrals involving stresses and velocities of one *unknown* flow field to the stresses and velocities of a *known* flow field. When only one quantity involving *integral* information is desired, e.g. force, torque, flow rate, etc., the 'reciprocal' approach often allows a solution to be obtained *without* determining the detailed velocity and stress fields of the actual problem under consideration. It is as if you are getting something for nothing. (I recall a visit to Howard Brenner in his MIT office and he had an old folder containing a seminar with this title.) As with many ideas, I was exposed to this idea in graduate and postdoctoral studies, but only began to appreciate it during the formative years of independent research while a young faculty member.

In low-Reynolds-number hydrodynamics these reciprocal ideas have been exploited for many years. Perhaps the first application was by Lorentz (1896). (For a collection of papers recognizing the centenary of this publication, as well as an English translation of Lorentz's paper, see Kuiken 1996.) The idea is central to the development of the boundary integral numerical method for viscous flows (e.g. Youngren & Acrivos 1975; Pozrikidis 1992). The mathematical steps are similar to Green's Theorems familiar from vector calculus, and related reciprocal identities are found in elasticity and electromagnetism. In the typical fluid mechanics problem involving the motion of particles or channel flows, the conjugate variables being related are force and particle velocity, torque and particle rotation rate, or flow rate and pressure drop. For an illustration of how the reciprocal approach is applied to prove symmetry properties of flow tensors relevant to low-Reynolds-number motions (see Hinch 1972).

The continuity and Stokes equations are $\nabla \cdot \boldsymbol{u} = 0$ and $\nabla \cdot \boldsymbol{\sigma} = \boldsymbol{0}$, where $\boldsymbol{u}$ and $\boldsymbol{\sigma}$ are, respectively, the velocity and stress fields. For a given geometry, i.e. the same domain with the same bounding surfaces S and unit normal $\boldsymbol{n}$ directed into the fluid, and considering a Newtonian fluid, it follows that the velocity and stress distributions, $\hat{\boldsymbol{u}}$ and $\hat{\boldsymbol{\sigma}}$, for a second viscous flow are related to $\boldsymbol{u}$ and $\boldsymbol{\sigma}$ by

$$\int_S \boldsymbol{n} \cdot \boldsymbol{\sigma} \cdot \hat{\boldsymbol{u}} \, \mathrm{d}S = \int_S \boldsymbol{n} \cdot \hat{\boldsymbol{\sigma}} \cdot \boldsymbol{u} \, \mathrm{d}S. \tag{2.1}$$

The quantity $\boldsymbol{n} \cdot \boldsymbol{\sigma}$ represents the force per unit area that the fluid exerts on the surface. Equation (2.1) is the starting point for applications of the Reciprocal Theorem to problems in low-Reynolds-number hydrodynamics; extensions are possible for the incorporation of inertial effects, viscoelastic features, etc.

2.1. *An application to a problem with a slip boundary condition*

As an illustration of the reciprocal approach to problems of recent interest in small-scale flows, we consider the influence of slip on the translation of a sphere of radius a in an unbounded fluid. In this problem there is a natural dimensionless parameter, λ/a, that enters the problem, where λ is the slip length; for a unidirectional flow adjacent to a stationary surface, λ is defined through the boundary condition $u = \lambda(\partial u/\partial n)$. The subject of slip has generated a large recent literature (e.g. Lauga, Brenner & Stone 2007), though the earliest theoretical ideas can be traced to Navier in 1823 (hence the terminology 'Navier slip length'). Although there is significant variation in experimental reports of slip, there appears to be a consensus emerging that indicate a slip length, even on solvophilic (solvent loving) surfaces, of the order of 10–30 nm. Note that for micron-sized objects, the slip effect is expected to be small,

$\lambda/a \ll 1$. Nevertheless, there are situations where the slip effect can be magnified by electric fields (e.g. Ajdari & Bocquet 2006). Here we investigate one consequence of hydrodynamic slip using the reciprocal approach; for examples of the electrokinetic enhancement investigated using the Reciprocal Theorem see Squires (2008).

To apply the Reciprocal Theorem, we consider as a 'test' problem $(\hat{\boldsymbol{u}}, \hat{\boldsymbol{\sigma}})$ the translation of a sphere of radius a with a no-slip boundary condition, i.e. $\hat{\boldsymbol{u}} = \hat{\boldsymbol{U}}$ on the sphere surface S_p, while the velocity decays at large distances. Stokes law give the hydrodynamic force $\hat{\boldsymbol{F}}^H = -6\pi\mu a\hat{\boldsymbol{U}}$ of the fluid on the sphere. It is a (very useful) fact of this classical solution that on the sphere's surface, the surface stress vector is $\boldsymbol{n}\cdot\hat{\boldsymbol{\sigma}} = -(3\mu/2a)\hat{\boldsymbol{U}}$, which is a constant.

Here we are interested in the force on the sphere with slip, $\boldsymbol{F}^H = \int_{S_p} \boldsymbol{n}\cdot\boldsymbol{\sigma}\,\mathrm{d}S$. Using the above results in (2.1), and recognizing that $\hat{\boldsymbol{U}}$ is an arbitrary vector yields

$$\boldsymbol{F}^H = -\frac{3\mu}{2a}\int_{S_p} \boldsymbol{u}\,\mathrm{d}S, \tag{2.2}$$

which only requires knowledge of the velocity distribution on the surface of the sphere. Also, the velocity decays at large distances, but on the surface of the sphere we must satisfy (i) the kinematic condition, $\boldsymbol{n}\cdot\boldsymbol{u} = \boldsymbol{n}\cdot\boldsymbol{U}$ and (ii) a slip condition, which is conveniently written in terms of the slip length λ and the surface stress. The two conditions may be written together using the surface projection operator $\boldsymbol{I} - \boldsymbol{nn}$:

$$\boldsymbol{u} = \boldsymbol{U} + \frac{\lambda}{\mu}(\boldsymbol{I} - \boldsymbol{nn})\cdot(\boldsymbol{n}\cdot\boldsymbol{\sigma}) \qquad \text{on } r = a. \tag{2.3}$$

The limit $\lambda = 0$ provides the no-slip condition and the limit $\lambda \to \infty$ is the case of a perfect slip surface, which is then supplemented with the kinematic condition.

Substituting (2.3) into (2.2) yields

$$\boldsymbol{F}^H = -6\pi\mu a\boldsymbol{U} + \frac{3\lambda}{2a}\int_{S_p} (\boldsymbol{I} - \boldsymbol{nn})\cdot(\boldsymbol{n}\cdot\boldsymbol{\sigma})\,\mathrm{d}S. \tag{2.4}$$

For $\lambda/a \ll 1$, it is natural to seek a perturbation expansion for the first effects of slip on the velocity and stress fields:

$$\boldsymbol{u}\left(\boldsymbol{r}, \frac{\lambda}{a}\right) = \boldsymbol{u}_0(\boldsymbol{r}) + \frac{\lambda}{a}\boldsymbol{u}_1(\boldsymbol{r}) + \cdots \quad \text{and} \quad \boldsymbol{\sigma}\left(\boldsymbol{r}, \frac{\lambda}{a}\right) = \boldsymbol{\sigma}_0(\boldsymbol{r}) + \frac{\lambda}{a}\boldsymbol{\sigma}_1(\boldsymbol{r}) + \cdots. \tag{2.5}$$

From the standpoint of the Reciprocal Theorem we note that the textbook, no-slip solution is simply the test case, $\boldsymbol{u}_0 = \hat{\boldsymbol{u}}$ and $\boldsymbol{\sigma}_0 = \hat{\boldsymbol{\sigma}}$.

In the limit $\lambda/a \ll 1$ we then approximate the integral in (2.4) using the stress fields based on the no-slip flow response, i.e. $\boldsymbol{n}\cdot\boldsymbol{\sigma} \approx \boldsymbol{n}\cdot\hat{\boldsymbol{\sigma}}$ is approximately a constant vector as explained above. Hence, noting that $\int_{S_p} (\boldsymbol{I} - \boldsymbol{nn})\,\mathrm{d}S = (8\pi/3)a^2\boldsymbol{I}$ we have directly from (2.4) that

$$\boldsymbol{F}^H \approx -6\pi\mu a\left(1 + \frac{\lambda}{a}\right)^{-1}\boldsymbol{U} \approx -6\pi\mu a\left(1 - \frac{\lambda}{a}\right)\boldsymbol{U}. \tag{2.6}$$

As expected physically, some slip on the sphere reduces the force. Most significantly, the result has been obtained without the need to calculate the detailed velocity distribution accurate to $O(\lambda/a)$.

For the more general case that the slip coefficient is piecewise constant on the surface of the sphere, there is the possibility of hydrodynamic coupling of rotation and translation, as described by Ramachandran & Khair (2009). This problem is

one of many variations of our basic example where we can take advantage of the Reciprocal Theorem (e.g. Leal 1980).

3. Free-surface thin-film flows: Landau–Levich–Derjaguin–Bretherton problems

Lubrication theory is commonly discussed in many textbooks though most do not hint at the great usefulness and applicability of the ideas. Traditionally, the topic concerns boundary-driven or pressure-driven flows of thin fluid films. Here 'thin' refers to the geometric characterization that the typical gap dimension h perpendicular to the flow direction is much smaller than the distance ℓ along which the flow occurs, i.e. $h/\ell \ll 1$. More precisely, the local slope cannot change too rapidly. Although most easily discussed for flows between rigid surfaces, which is the usual application of 'lubrication', the ideas find many research applications in flows involving free-surface thin-film flows (e.g. Oron, Davis & Bankoff 1997). Thus, 'lubrication' ideas apply to coating processes, film levelling, liquid spreading, etc. One large class of problems concerns driven coating flows of perfectly wetting liquids that have in common the influence of surface tension on the formation of a thin film of uniform thickness (often only a few microns) from a meniscus region of much larger length scale (generally millimetres to centimetres). For a brief overview of the kinds of problems impacted by capillary phenomena (see Pomeau & Villermaux 2006).

3.1. *A large class of common coating flows*

Five traditional problems of this thin-film type are shown in figure 5(a–e). Figure 6 shows two that are less familiar, having a similar structure, that will be discussed in § 3.4. We exhibit in figure 5(a) the coating of a plate as it is drawn vertically with speed U from a fluid of viscosity μ and density ρ, where γ is the surface tension and g denotes the acceleration of gravity. Gravitational effects try to maintain a flat interface while viscous effects cause withdrawal of a film of liquid. Our goal is to determine the thickness of the film h_∞ as a function of the physical parameters ρ, g, γ, μ and U. Figure 5(b) illustrates the similar problem for coating a fibre of radius b. These coating-flow problems, which are the two classical problems of coating theory, were first analysed by Landau and Levich (1942) for withdrawal of a plate and by Derjaguin (1943) for a fibre.

In addition, figure 5(c) shows a rotating horizontal cylinder partially immersed in a bath of liquid where the rotation generates a thin film along the top of the surface of the rotating cylinder (Tharmalingam & Wilkinson 1978). This configuration is encountered in fibre coating processes where, for example, a fibre can be drawn through the thin film. Figure 5(d) illustrates the next of the traditional problems, namely a long gas bubble propagating through a circular tube where it is separated from the boundary by a thin film; this configuration was first analysed by Bretherton (1961) (see also Ratulowski & Chang 1990). In one version of the problem there is a pressure-driven flow in the tube and we are interested in the speed of the bubble relative to the liquid. It turns out that the speed is related to the thickness of the thin film, and so makes a close connection to the other problems shown in figure 5.

A final problem of this thin-film type concerns coating the inside of a horizontal rotating cylinder (figure 5e) that contains a pool of liquid at its bottom (Ashmore *et al.* 2003; Tirumkudulu & Acrivos 2001). In all of the five cases sketched in figure 5(a–e), so long as both an effective Reynolds number and an effective capillary number (which compares viscous stresses to surface tension stresses) are small, there is a nearly static meniscus of constant curvature that is connected to a thin film whose

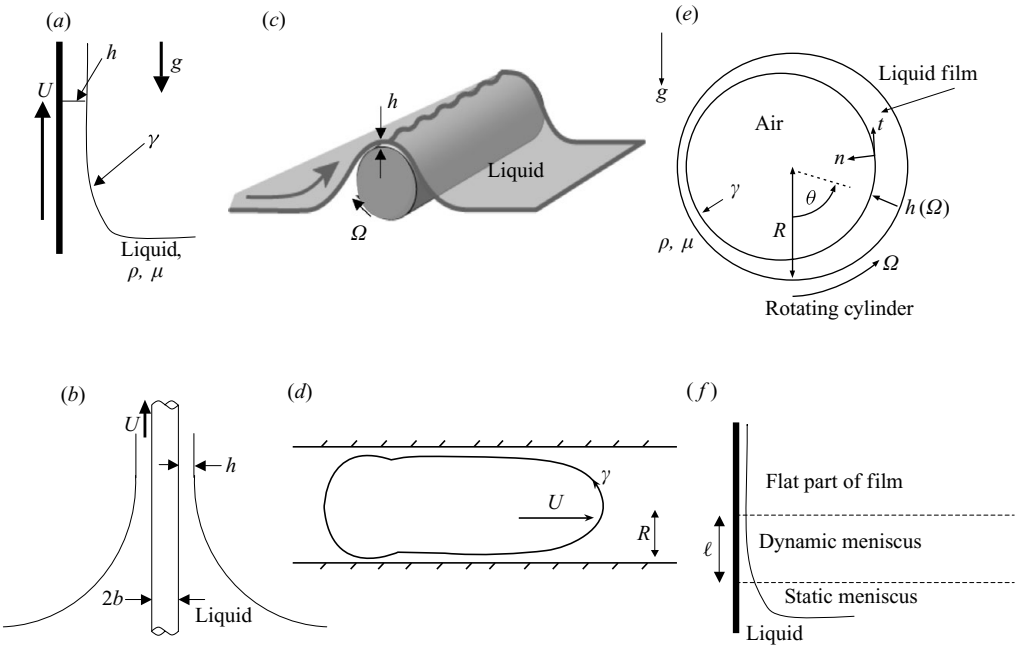

FIGURE 5. The Landau–Levich–Derjaguin–Bretherton class of coating flows. (*a*) Coating a plate by vertical withdrawal from a bath of liquid. (*b*) Coating a fibre of radius *b* by withdrawal from a bath of liquid. (*c*) Roll coating of a horizontal rotating cylinder partially immersed in a bath of liquid. (*d*) Motion of a bubble in a liquid-filled tube of radius *R* (Bretherton 1961). (*e*) Coating the inside of a hollow horizontal rotating cylinder partially filled with liquid (Ashmore, Hosoi & Stone 2003). (*f*) Schematic indicating the approach towards thinking about thin-film free-surface flows involving moving substrates (after Fanton, Cazabat & Quéré 1996).

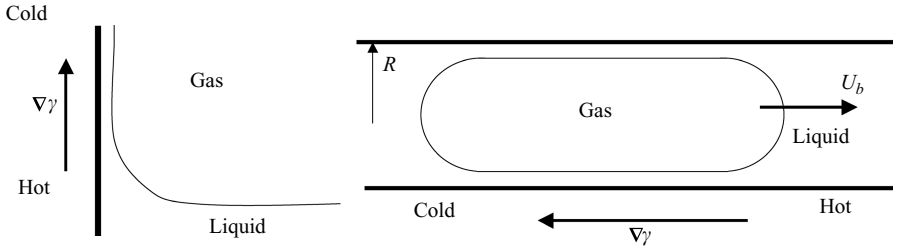

FIGURE 6. Thermocapillary-driven coating flows. (*a*) Coating a plate by application of a vertical temperature gradient along the plate. (*b*) Translation of a bubble in a tube driven by a temperature gradient along the tube.

thickness is established by dynamical effects. The goal is to calculate the shape of the film and the constant film thickness far from the meniscus.

We shall see that these distinct thin-film flow problems are, in fact, basically the same from a fluid dynamical perspective – in recognition of this similarity, we refer to these as LLDB problems (e.g. see de Gennes, Brochard-Wyart & Quéré 2003). It is important to realize that the film thickness is not known *a priori*, but rather it is a quantity that must be determined as part of the solution to the problem. Below we also show how an understanding of the structure of the LLBD problems makes it

possible to identify the basic scaling results in similar geometrical problems generated by thermocapillary flows.

The remarkable fact is that all five problems (figure 5*a–e*) share a common solution for the thickness h_∞ of the uniform film region of the form:

$$\frac{h_\infty}{\ell_m} = c_1 \left(\frac{\mu U}{\gamma}\right)^{2/3} = c_1 \mathscr{C}^{2/3}, \tag{3.1}$$

where ℓ_m denotes the radius of curvature of the meniscus from which the film is withdrawn. Here $\mathscr{C} = \mu U/\gamma$ is the capillary number, which must be small (typically less than 10^{-2}) for the analytical solution to be a good approximation. The $O(1)$ prefactor is known from solving an ordinary differential equation: $c_1 = 1.337$. For example, the length scale $\ell_m = \ell_{\rm cap}/\sqrt{2}$, where the capillary length $\ell_{cap} = \sqrt{\gamma/\rho g}$ is the relevant length scale for plate coating, $\ell_m = b$ for coating of a fibre of radius b and $\ell_m = R$ for the movement of a bubble in a tube of radius R. For the case of coating the horizontal cylinder of radius R, we have that ℓ_m is proportional to the smaller of ℓ_{cap} and R (Tharmalingam & Wilkinson 1978), while for coating the inside of the cylinder, ℓ_m depends on the amount of fluid in the bottom (Ashmore *et al.* 2003). This brief summary makes clear that the nontrivial scaling with capillary number in (3.1) makes many appearances in the coating flows literature!

I still recall the first time that I studied this result in the classical book *Physicochemical Hydrodynamics* by Levich (1962), though I no longer remember what sent me looking there; the reader may also wish to consult the text of the same title by Probstein (1994). The elegance of the solution made a particularly strong impression on me since in the case of a plate withdrawn from a liquid bath we expect the film thickness $h_\infty = f(U, \rho, \mu, g, \mu, \gamma)$, which is a relationship among six variables. Dimensional analysis lets us conclude that the film thickness is characterized by three dimensionless parameters. However, for small Reynolds and Bond numbers, we can deduce that the film thickness, relative to a characteristic length, is a function of the capillary number. In the case of plate withdrawal, the meniscus is characterized by a radius of curvature given by the capillary length, $\ell_m = (\gamma/(2\rho g))^{1/2}$, so that with the assumptions mentioned above, (3.1) yields

$$h_\infty = 0.946 \frac{(\mu U)^{2/3}}{(\rho g)^{1/2}\, \gamma^{1/6}}. \tag{3.2}$$

This result involves three distinct power laws! This nontrivial result, first derived by Landau and Levich, grabs your attention! For a summary of other coating flow problems, see the review paper by Quéré (1999). In addition, there are cases where films can be thicker than the prediction of (3.1) as discussed by Snoeijer *et al.* (2008).

From the historical perspective of problem solving in fluid dynamics and applied mathematics, I also find it interesting that the solution procedure utilized by Landau and Levich was essentially a boundary-layer calculation, or what we would more formally call a solution using singular perturbation theory. The solution requires matching of an inner region – the dynamical thin film – to an outer region – the static meniscus (Wilson 1981). This solution is completed by demanding that the curvatures match in an overlap region. Of course, at the time of the original publication there was no systematic procedure for treating such problems so Landau and Levich proceeded, absolutely correctly, on physical grounds.

3.2. *The origin of the LLDB scaling*

As with any specialized topic, (3.1) is 'well known to those that know it well'. Although this paper is not the place to give a detailed derivation, it is useful to indicate, via order-of-magnitude arguments, the origin of this scaling result for h_∞. We will see in § 3.4 that the ideas then allow us to understand other related thermocapillary flow problems. There are three steps that build on the idea that the flow can be considered to have both a dynamical thin-film region of unknown length scale ℓ along the flow direction, where the lubrication approximation describes the viscous flow, and a static regime, where the curvature of the meniscus region is established. At several steps the approximation $h_\infty/\ell \ll 1$ is used.

The basic ideas are:

(i) In the thin film region the interface is curved, with a typical curvature, $O\left(h_\infty/\ell^2\right)$, so that the capillary pressure in the liquid is $p \approx -\gamma h_\infty/\ell^2$ (relative to the ambient pressure).

(ii) A lubrication analysis of the thin-film flow gives a fluid velocity u along the film that satisfies (ignoring signs)

$$\frac{\mu u}{h_\infty^2} \approx \frac{\Delta p}{\ell} \approx \frac{\gamma h_\infty}{\ell^3}. \tag{3.3}$$

This result expresses a balance between a boundary-driven viscous flow and a pressure-driven suction flow generated by the curved meniscus. The basic momentum balance is quite general, e.g. in lubrication flows it is always true that the pressure drop Δp and the velocity along the flow direction are related by $\Delta p \approx \mu u \ell/h_\infty^2$. Therefore with $u = O(U)$ for the viscous withdrawal problem (figure 5*a*), or $u = U_b$ for the speed of the bubble (figure 5*d*), then according to (3.3) we have the order-of-magnitude estimate

$$\left(\frac{h_\infty}{\ell}\right)^3 \approx \mathscr{C}, \tag{3.4}$$

where $\mathscr{C} = \mu U/\gamma$ (replace U by U_b for the case of a bubble). This result supports the self-consistency of the lubrication approximation for the flow since $h_\infty/\ell \ll 1$ provided $\mathscr{C} \ll 1$; a detailed study makes clear that the solution is an expansion in the capillary number.

Those readers familiar with the dynamical contact angle for wetting liquids will recognize the relationship in (3.4) of the capillary number to the cube of the ratio of length scales. For example, Tanner's law for the dynamical contact angle θ_d of a perfectly wetting liquid is $\theta_d^3 \propto \mathscr{C}$ (de Gennes 1985); see also a discussion of the logarithmic correction to (3.4) by Eggers & Stone (2004).

(iii) The shape of the thin film must evolve to have a curvature comparable to the static meniscus, $h_\infty/\ell^2 \approx 1/\ell_m$. We thus identify $\ell = O\left(h_\infty \ell_m\right)^{1/2}$, which, when substituted into (3.4), yields the form of (3.1).

In this way, for standard coating flow problems, we can always understand the thickness of the thin film as a function of the speed and material parameters. We also take the opportunity to indicate other connections that follow naturally once this point is appreciated. For example, for a drop spreading by capillary forces on a plane where the drop has typical time-dependent height $h(t)$ and breadth $R(t)$, $h/R \approx \tan\theta_d$. Hence, using $\theta_d^3 \propto \mathscr{C}$, then for the two-dimensional problem, where $hR = \text{constant}$, we take $\ell = R$ and since $u \approx R/t$ we obtain the well-known scaling dynamics $R \propto t^{1/8}$. Similarly, for the axisymmetric spreading of a drop $hR^2 = \text{constant}$

and we find $R \propto t^{1/10}$ (Tanner's law). Note that there are important details and ideas that this heuristic overlooks.

3.3. *Completing the bubble problem: the relative speed of the bubble to the fluid*

We noted with respect to figure 5(d) that, when a bubble moves in a liquid-filled tube, the relative speed of the bubble is linked to the film thickness. Here we consider a bubble moving due to a pressure-driven parabolic flow in a circular tube of radius R. We consider a mass balance in the frame of reference fixed to the bubble. Now, let U_b denote the bubble speed and $\langle U \rangle$ denote the average speed of the liquid. Then, within the thin-film approximation,

$$(\langle U \rangle - U_b)\pi R^2 = -2\pi R h_\infty U_b \quad \text{or} \quad \frac{U_b - \langle U \rangle}{U_b} = \frac{2h_\infty}{R} \propto \left(\frac{\mu U_b}{\gamma}\right)^{2/3}. \tag{3.5}$$

When the capillary number is small, the bubble moves a little faster than the mean speed of the liquid. This result is in excellent agreement with numerical simulations and experiments on clean systems. Surfactant effects typically modify the prefactor (e.g. Ratulowski & Chang 1990; Quéré 1999).

As a final remark on the problem of a translating bubble, we note that these results have been generalized to the case of bubbles in polygonal capillaries (Wong, Radke & Morris 1995*a*,*b*) where liquid flow in the corners needs to be considered. For these systems, experiments show that surfactants modify the results significantly, so that the bubbles may move more slowly than the mean liquid flow because of a substantial corner effect (Fuerstman *et al.* 2007).

There is a small but important feature that leads to improved agreement with experiments when the capillary number is increased. Accounting for the film thickness, the radius of curvature of the end of the bubble is changed to $O(R - h_\infty)$. It is straightforward to modify step (iii) above so that $\ell \approx (h_\infty R)^{1/2}(1 - h_\infty/R)^{1/2}$, which yields a modified approximation for the Bretherton problem commonly expressed as $h_\infty/R = c_1\mathscr{C}^{2/3}(1 - 2.5c_1\mathscr{C}^{2/3})^{-1}$, as was first given by (Aussillous & Quéré 2000). In this case, the film thickness is reduced relative to the LLDB prediction.

3.4. *Thermally driven thin films*

In recent years there has been substantial interest in driving fluid motions using surface tension gradients. We generally speak of such flows as driven by Marangoni stresses (Scriven & Sternling 1960). For example, it is well known that the interfacial tension can be generally decreased with increasing temperature or by adding surfactants. Such gradients produces tangential stresses along a fluid–fluid interface that always lead to fluid motion. The thermocapillary effect $\gamma(T)$ with $\mathrm{d}\gamma/\mathrm{d}T < 0$ in most cases, has been used to control fluid motions.

We give two examples that will remind us of the thin-film flows in figure 5. First, figure 6(a) shows a schematic where a linear temperature gradient along a plate drives a thin fluid film towards the lower temperatures or higher surface tensions (e.g. Fanton, Cazabat & Quéré 1996; Kataoka & Troian 1999). This example is representative in that the temperature gradient applied along a substrate is essentially imprinted on the interface since the liquid film is thin. The question to be answered what relates the film thickness to the driving force, which is the temperature gradient, and to the material properties. In addition, figure 6(b) illustrates the same idea for driving a gas bubble along a liquid-filled channel (Mazouchi & Homsy 2000).

Obviously, there are similarities of these problems to other surface-tension-driven flows. For example, the thin-film flow along a plate brings to mind wine tears, which

are driven by a chemical Marangoni effect (e.g. Hosoi & Bush 2001). The first steady thermocapillary flow of this type was the movement of a bubble in a prescribed temperature gradient in an unbounded bath of fluid, which was analysed by Young, Block & Goldstein (1959). In this case, the liquid is dragged towards the higher tension regions and thus the bubble 'swims' towards higher temperatures.

We now proceed to give the main scaling results for the problems in figure 6, building on the basic results we learned from the LLDB scaling. If the temperature distribution along the surface (e.g. $T(s)$) is assumed to be linear, with gradient $\mathrm{d}T/\mathrm{d}s = G > 0$, then the gradient of surface tension $G|\mathrm{d}\gamma/\mathrm{d}T| = \tau$ yields a constant applied surface stress. We shall treat τ as given. These stresses act to pull liquid towards regions of higher surface tension (figure 6*a*), while we assume the usual capillary effects associated with pressure-driven suction flow towards the meniscus can still be approximated using an average value of the surface tension γ_0. At the interface, the thermocapillary stresses τ balance the viscous stresses $O(\mu U_T/h_\infty)$, where U_T is the thermocapillary speed along the surface of a film of thickness h_∞. Hence, the corresponding velocity of the fluid relative to the stationary substrate is $U_T \approx h_\infty \tau/\mu$. The basic ideas behind the classical Landau–Levich–Derjaguin–Bretherton result (see (3.1)) then apply and so we expect a film thickness in thermocapillary flows, due to the applied stress τ, with order of magnitude

$$h_\infty \approx \ell_m \left(\frac{\mu U_T}{\gamma_0}\right)^{2/3} \approx \ell_m \left(\frac{h_\infty \tau}{\gamma_0}\right)^{2/3} \quad \Rightarrow \quad h_\infty \approx \frac{\ell_m^3 \tau^2}{\gamma_0^2}. \tag{3.6}$$

We thus observe that the film thickness h_∞ is a strongly increasing function of the applied surface shear stress τ. This result was first obtained by Fanton, Cazabat & Quéré (1996), who also confirmed it experimentally.

The scaling result (3.6) is also *exactly* what is obtained when considering the thermocapillary motion of a bubble through a tube of radius R (Mazouchi & Homsy 2000), as displayed in figure 6(*b*). When the bubble translates, there is a thin film separating the gas–liquid interface from the boundary and this film has a thickness given by (3.6). As in § 3.3, a mass balance yields $U_b \pi R^2 = U_T 2\pi R h_\infty$, so that we obtain (take $\ell_m = R$)

$$U_b \approx \frac{2U_T h_\infty}{R} \propto \frac{\tau h_\infty^2}{\mu R} \propto \frac{\tau^5 R^5}{\mu \gamma_0^4}. \tag{3.7}$$

This result was obtained originally from a detailed calculation by Mazouchi & Homsy (2000). We observe that the bubble speed is a particularly strong function of τ, R and γ_0. The relation of these two thermocapillary flow problems to each other, and more generally to the basic LLDB flow problems, illustrates the unifying features that tie together many forced coating flows.

4. Nearly two-dimensional viscous flows

If the Reynolds number is small, there is a conundrum when solving the Navier–Stokes equations for steady, unbounded two-dimensional motions; this fact is known as the Stokes paradox (e.g. Leal 2007). In particular, if the inertia terms in the Navier–Stokes equations are neglected entirely, then there is no solution to the two-dimensional velocity field representative of a cylinder of radius a translating perpendicular to its long axis with velocity $\boldsymbol{U}$ (figure 7*a*). One hint that the problem, as posed, is unusual can be obtained from dimensional analysis for the force per unit length, f, on the cylinder: in the low-Reynolds-number limit $\boldsymbol{f}$ should depend on

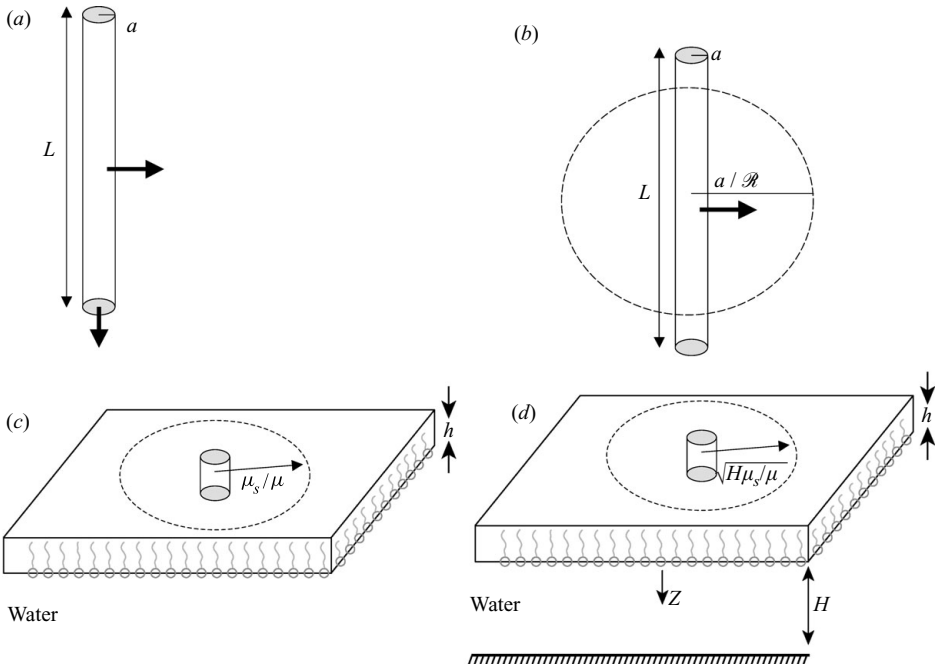

FIGURE 7. Nearly two-dimensional flows. (*a*) Translation of a slender particle transverse to its long axis. (*b*) Schematic indicating the distance $a/\mathscr{R} < L$ at which inertial effects enter when the Reynolds number is small. (*c*) Translation of an object in a bilayer or along a thin sheet of viscous liquid. An indication is given of the length scale μ_s/μ at which the flow outside the membrane impacts the motion, where μ_s is the surface viscosity and μ the viscosity of the surrounding liquid. (*d*) The motion in a bilayer can be influenced by flow in the surrounding subphase when the depth $H < \mu_s/\mu$.

μ, $\boldsymbol{U}$ and a, and so we reach the conclusion that $\boldsymbol{f} \propto \mu\boldsymbol{U}$, and is independent of the cylinder radius, which seems physically unrealistic. It turns out that this basic problem of the drag on a translating cylinder in a low-Reynolds-number flow captures ideas that occur in other viscous flow problems that are nearly two-dimensional. Sketches of such problems are given in figure 7 and are further discussed below; similar mathematical ideas occur in a variety of problems in potential theory.

For a terse, insightful discussion of the resolution of the Stokes paradox, including the first effects of inertia on the flow due to a translating cylinder (see Batchelor 1967). In the Stokes limit, an analysis of the two-dimensional flow past a cylinder shows that the velocity varies logarithmically with distance $\boldsymbol{r}$ from the cylinder, $\boldsymbol{u}(\boldsymbol{r}) \approx \boldsymbol{U}\,(1 + c\ln(r/a))$, where c is a constant. This logarithmic response plagues many two-dimensional problems in fluid dynamics, elasticity and electromagnetism.

Although many of the details of these problems are complicated there is a very useful order-of-magnitude estimate that is worth remembering and which follows from the logarithmic variation of the velocity distribution. In most cases we expect that the velocity variations about an object occur on a geometric length scale, such as the radius of the cylinder. Hence, for an object of radius a, we are typically taught to estimate the velocity gradient as $|\nabla\boldsymbol{u}| = O\,(U/a)$. However, now we observe that in nearly two-dimensional viscous flows, because of the appearance of the logarithmic factor, the velocity variations occur over a length scale longer than the radius. When a viscous fluid motion is nearly two-dimensional so that a logarithmically varying

Flow problem	Force/length
Cylinder translating parallel to its axis, $\mathscr{R}=0$	$\dfrac{2\pi\mu U}{\ln(0.3L/a)}$
Cylinder translating perpendicular to its axis, $\mathscr{R}=0$	$\dfrac{4\pi\mu U}{\ln(0.82L/a)}$
Cylinder translating perpendicular to its axis, $\mathscr{R}<1$	$\dfrac{4\pi\mu U}{\ln(3.7/\mathscr{R})}$
Drag on a cylinder in a square array, array fraction $\phi \ll 1$	$\dfrac{4\pi\mu U}{\ln(0.48/\phi^{1/2})}$
Disk translating in a membrane, infinite surroundings on both sides	$\dfrac{4\pi\mu_s U}{\ln(0.56\mu_s/(\mu R))}$
Disk translating in a membrane near a rigid boundary H away	$\dfrac{4\pi\mu_s U}{\ln(1.1(\mu_s H/(\mu R^2))^{1/2})}$

TABLE 1. A summary of the force per unit length on cylindrical-like bodies in various nearly two-dimensional flows. Here L is the end-to-end length of a cylinder of radius a, which is translating at speed U. The Reynolds number is here defined in terms of the translation speed U as $\mathscr{R}=\rho U a/\mu$. The first entry is given by Batchelor (1967, p. 246). The second and third entries are given by Lighthill (1975, p. 62). The fourth entry concerns the drag on a cylinder in a fixed array, where ϕ represents the area fraction of the cylinders (e.g. Sangani & Acrivos 1982; Koch & Ladd 1997). The final two entries concern the force objects (radius R) translating in viscous membranes (surface viscosity μ_s) in the limit $\mu_s \gg \mu R$ and the last entry further assumes that the drag is dominated by the nearby boundary a distance H away.

velocity is expected, the velocity gradients occur on a length $a\ln(\ell/a)$, where $\ell > a$ is a length at which the two-dimensional character of the flow is changed. The length ℓ effectively distinguishes between solutions of different problems such as those shown in figure 7. In these cases, it is convenient to work with the approximation $|\nabla \boldsymbol{u}| = O\,(U/(a\ln(\ell/a)))$.

For a cylinder of length L and radius a, with $L \gg a$, translating perpendicular (or parallel) to its axis (figure 7*a*), the flow is three-dimensional at the scale of L, so $\ell \propto L$ (Lighthill 1975). We then estimate the force per length, $\boldsymbol{f}$ on the translating cylinder as the product of the shear stress and the perimeter, or

$$\boldsymbol{f} \approx O\left(\frac{\mu \boldsymbol{U}}{a\ln(\ell/a)}2\pi a\right) \approx O\left(\frac{2\pi\mu \boldsymbol{U}}{\ln(c_2 L/a)}\right), \tag{4.1}$$

for some constant c_2.

Similarly, when we consider the influence of inertial effects on the motion of a cylinder of length L and radius a translating at speed U, we first define a Reynolds number $\mathscr{R}=\rho U a/\mu$. We consider $\mathscr{R} \ll 1$. Then, the distance ℓ at which a viscously dominated flow decays sufficiently for inertial effects to be significant is $\ell \propto a\mathscr{R}^{-1}$; this length scale is most commonly referred to as the Oseen length. Hence, the force/length for a translating cylinder is proportional to $\mu \boldsymbol{U}/\ln(c_3/\mathscr{R})$, for some constant c_3.

These ideas for the drag on objects are important when we consider below (briefly) the movement of objects in cell membranes and other viscous films (figure 7*c*, *d*). A summary of results applicable to nearly two-dimensional viscous flows, given in terms of the force/length on an object, are given in table 1. A further example, which John Brady pointed out to me, is low-Reynolds-number flow through arrays of cylinders; here the cutoff length is $\ell \propto \phi^{-1/2}$ where ϕ is the (small) area fraction of cylinders.

The two facts to take away from the above discussion are that the force/length is proportional to $\mu \boldsymbol{U}$ (dimensional analysis) and varies inversely with $\ln(\ell/a)$, where ℓ is a problem-dependent length scale.

5. The viscosity of thin films and interfaces

Complex fluids refer to the area of fluid dynamics research where suspended objects in the fluid, e.g. rigid particles, bubbles and drops, cells, vesicles, micelles, polymers, etc., or interfaces, e.g. surfactant covered surfaces, thin liquid films, membranes of some type, etc., make a substantial impact on, or even control, the fluid motion. The subject appears in many guises and crosses traditional scientific boundaries. In my research group we have studied a number of questions from which emerged common themes associated with the importance of such interfaces. As is often the case, hindsight has made it easier to see the connections.

5.1. *Diffusion in biological membranes*

In the early 1970s biologists discovered that the bilayer membrane of a cell, which is often visually depicted with the phospholipid molecules in a nice orderly packing, is in fact much more fluid-like. The lipids, and objects such as integral membrane proteins, diffuse relatively freely (Singer & Nicholson 1972); a more up-to-date understanding of the fluid mosaic model is by Jacobsen, Sheets & Simson (1995). A natural fluid mechanics question to ask is 'what is the diffusivity of an object in a fluid membrane?' Following the traditional description of Brownian motion given by Einstein in 1905, we expect that the diffusion coefficient is $D = k_B T/(F/U)$, where F is the force needed to translate the object at speed U. Therefore, the basic question arises as to the force–velocity relation for an object in a fluid membrane.

At these scales the dynamics are those of low Reynolds numbers. Moreover, a common way of thinking about the dynamics is to consider the membrane as a viscous fluid layer of viscosity μ_m and thickness h as in figure 7(*c*); physical chemists commonly refer to the surface viscosity $\mu_s = \mu_m h$. Let μ denote the viscosity of the fluid surrounding the membrane. Because the objects are generally depicted as cylinders translating in a plane, the answer to this question is complicated by the well-known Stokes paradox, as discussed in § 4, which tells us that there is no solution to the steady translation of a cylinder. Nevertheless, Saffman and Delbrück effectively answered the question of how to calculate the diffusivity of an object in a fluid membrane (Saffman & Delbrück 1975). A complete fluid mechanical description, resolving the paradox by accounting for the fluid surrounding the membrane, was given in a classic paper by Saffman (1976).

As a personal note, at Philip Saffman's retirement party, which was held at his home in Pasadena, I asked him during a quiet moment when he was alone in his front yard, if he had worked with Delbrück because Caltech was such a small, collegial place. As I recall he simply turned and pointed to the house next door, and said something like, 'Well, the real reason was that Max Delbrück ... lived next door. We used to mow the lawn together, rake the leaves together ...'.

Saffman considered the translation of a membrane-bound object, radius R, which spans the thickness h of the membrane, as sketched in figure 7(*c*). To evaluate the force on the object, consider the drag from the fluid flow around it; the drag has magnitude $O(\mu_m U h)$. In addition, there is drag from the subphase that lies either on one or both sides of the membrane; this contribution to the drag has magnitude $O(\mu U R)$. Therefore, a dimensionless parameter, often referred to as the Boussinesq

number, for the description of the motion is

$$\mathscr{B} = \frac{\mu_m h}{\mu R} = \frac{\mu_s}{\mu R}. \tag{5.1}$$

Note that we have used the surface viscosity $\mu_s = \mu_m h$, which characterizes the viscosity of a two-dimensional sheet. The ratio μ_s/μ is a length scale and effectively represents the distances in the membrane over which the flow is approximately the two-dimensional flow about a cylinder and beyond which the drag from the surrounding fluid causes a rapid decay of the velocity disturbance. Thus, for lipid molecules $\mu_s/\mu > h$, which was the limit of interest to Saffman and Delbrück, we expect a force/length ratio on the cylinder comparable to the case of cylinder in a viscous fluid (see table 1), where now the logarithmic correction is cutoff on the length scale $\ell = \mu_s/\mu$. Thus, the drag force on a membrane-spanning object is

$$\boldsymbol{F} = -\frac{4\pi\mu_s \boldsymbol{U}}{\ln(2\mu_s/\mu R) - \gamma_E} = -\frac{4\pi\mu_s \boldsymbol{U}}{\ln(0.56\mu_s/\mu R)}, \tag{5.2}$$

where $\gamma_E = 0.5772\ldots$ is Euler's constant.

For much larger objects such as phase-separated lipid domains of radius R in the membrane (such domains can be tens to hundreds of microns in size), we have $\mu_s/\mu < R$. I first learned about these systems via a collaboration with Harden McConnell of Stanford University who introduced me to these kinds of questions concerning the fluid mechanics of membranes. In particular, McConnell encouraged me to think about the influence of nearby substrates simply because so many experiments involve microscope slides. (I worked closely with McConnell for a few years, and it was a great experience. He is one of the leading chemists and scientists of his generation and is an inspiring collaborator. One day one of his graduate students sent me an email saying that they had just completed a group meeting during which McConnell said 'Physical chemistry was invented by nice people, biology was invented by God, and fluid mechanics was invented by the devil.') Hence, we considered the translation of a domain of radius R in a membrane with a rigid substrate a distance H away, as sketched in figure 7(d) (Stone & Ajdari 1998). For example, for the case where $\mu_s/\mu > R$, but for which the boundary effects are significant, implying $\mu_s/\mu > R > H$, we found that the flow should be nearly two-dimensional, with a cutoff distance set by the length $\ell = \sqrt{(\mu_s H/\mu)}$. Hence, in this limit we obtain the drag force

$$\boldsymbol{F} = -\frac{4\pi\mu_s \boldsymbol{U}}{\ln\left(1.1(\mu_s H/\mu R^2)^{1/2}\right)}, \tag{5.3}$$

where the constant in the logarithm is modified by a factor 2 since in this limit, only the drag from the thin film on one side of the object effectively matters.

Surfactant-covered interfaces also offer an added resistance to fluid motion (e.g. Scriven 1960; Edwards, Brenner & Wasan 1991). One method for probing the rheology of such interfaces is to use the above results, or closely related extensions, but applied to particles purposely added to the interface (see Cheung *et al.* 1996; Sickert, Rondelez & Stone 2007). Measuring the Brownian movement of individual particles allows the surface viscosity to be estimated.

As this section should make clear, this class of fluid dynamics problems concerning the flow within interfaces is a nice example of how hydrodynamic ideas are useful for providing quantitative estimates to biological and rheological questions. It is a case involving an interface at the interface of disciplines.

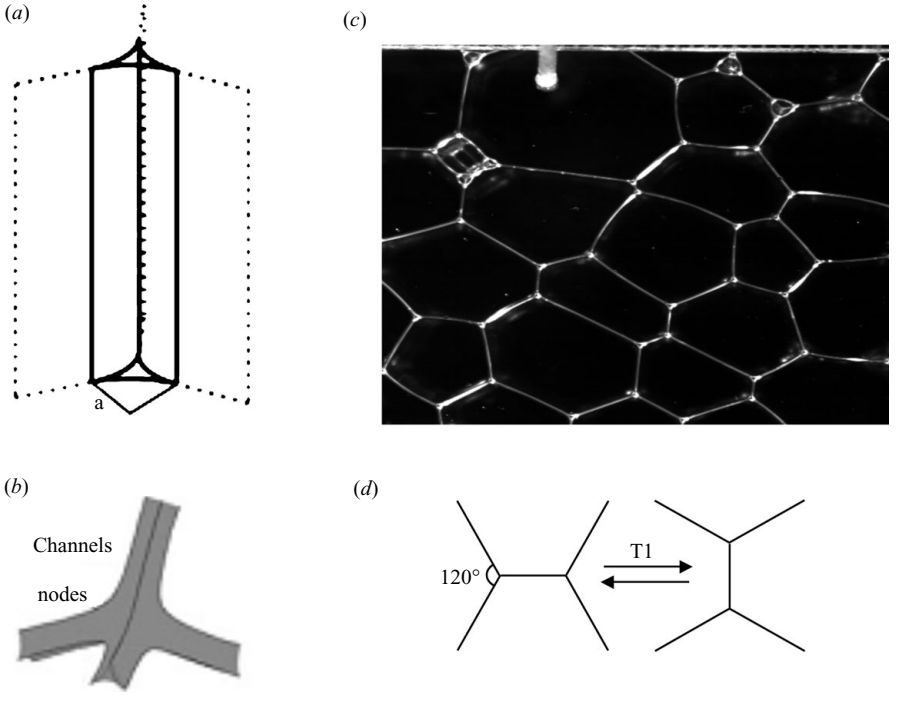

FIGURE 8. Dynamics associated with interfaces impact flows and rearrangements in foams. (*a*) In a foam with low liquid fractions, the liquid resides in a channel-like network, where (*b*) four channel channels meet in junctions. (*c*) In a two-dimensional foam trapped between glass plates, rearrangements of the bubbles typically occur by (*d*) shortening of individual sides that then lengthen in such a way that bubbles switch neighbours, which is known as the T1 process.

5.2. *Surfactant-stabilized thin films*

We close with two examples highlighting the importance of properties of the interface for dictating dynamics of fluid flows. As is familiar to all of us, shaking a bottle of soapy water produces a foam. There are many fluid mechanical questions that arise when thinking about foams and soap films (see Mysels, Shinoda & Frankel 1959; Weaire & Hutzler 1999). For example, over time the structure of the foam changes: (i) liquid drains from the foam due to gravity (surface tension effects tend to resist the drainage); and (ii) the typical bubble size increases as either gas diffuses from small to large bubbles or the films between the bubbles ruptures following a gradual thinning process (coarsening).

What factors influence the drainage rate? For the limit that the liquid volume fraction is small, most of the liquid resides in a channel-like network (Plateau borders), and the liquid flow is modelled as in a network of channels (figure 8*a*, *b*). Consequently the drainage rate of liquid from the foam is established both by the structure of the foam (bubble size, liquid fraction), which sets the geometric dimensions of the channels, as well as the type of surfactants, which establishes boundary conditions for the flow in the channel-like network. Resistance is associated with flow along the long sections of the Plateau border (figure 8*a*) when the interfaces are nearly rigid (Weaire & Hutzler 1999) and the nodes or junctions (figure 8*b*) where velocity gradients remain significant even when the interfaces are mobile

(Koehler, Hilgenfeldt & Stone 1999). In fact, most experimental data lie between these two limits. Accounting for the effects of surface viscosity along the surfaces of the Plateau borders (first described by Leonard & Lemlich (1965)) provides a systematic means, dependent on the type of surfactant, for interpolating between the two limit cases (Koehler, Hilgenfeldt & Stone 2004; Koehler *et al.* 2004). Thus, the interfacial properties dictate the drainage rate.

Our final example concerns the time needed for spontaneous rearrangements in a foam. The simplest case is a dry foam trapped between two transparent plates, where the bubbles span the gap (figure 8*c*). This example is frequently on display in museums. In such a two-dimensional setting the minimum energy configuration is a perfect hexagonal tiling of equal size bubbles. Consequently, any initial state that is different is constantly evolving to lower energy configurations and it does so by films shortening, then switching neighbours and suddenly rearranging, which is called the T1 process (see figure 8*d*). What is the typical time of such a rearrangement?

We investigated this question using controlled experiments to trigger the instability (Durand & Stone 2006). By changing the bulk viscosity of the solution μ and the type of surfactant we showed that the dynamics were independent of μ but depended strongly on the surfactant type, i.e. on the surface viscosity μ_s. On dimensional grounds then there is a time scale related to the driving force for area minimization, i.e. the surface tension (γ), and the interfacial resistance (μ_s), which suggests the rearrangement time scale is proportional to μ_s/γ. In our experiments, $\mu_s \approx 30 \times 10^{-3}\,\mathrm{N\,s\,m^{-1}}$ and $\gamma \approx 30 \times 10^{-3}\,\mathrm{N\,m^{-1}}$, so there is a time scale about 1 s, which is the order of magnitude that was observed experimentally.

6. Closing remarks

Fluid dynamics is a subject that is inspiring in its breadth of applicability. Here we have described a set of problems that occur when fluid–fluid interfaces participate actively in the dynamics. That the topics occur also at the interface of disciplines is especially educational and where these topics can lend insight into problems of some practical importance is particularly gratifying.

In closing, I think it is important that as a community we do more to participate in educational initiatives, since fluid mechanics can help inspire many learning experiences, and to identify and work on technical problems of value to industry and society, especially since fluid mechanics, in many guises, appears abundantly in ways that matter. The new topics that arise also refresh our discipline. On a more personal note, our studies allow us to interact internationally and that is a facet of my work that I continually treasure.

I earned an undergraduate degree in Chemical Engineering at UC Davis, where the educational environment was outstanding, and where I was first exposed to fluid mechanics and transport processes. Gary Leal at Caltech, and Caltech itself, provided a great environment to undertake basic research in fluid mechanics. I was given wonderful opportunities to learn and meet first hand many ideas and people: Philip Saffman was active in the Applied Mathematics program and Julio Ottino, in the middle of formulating his thinking about mixing, visited Caltech for an extended time during my final year. I then had an opportunity to work with John Hinch at DAMTP, and benefitted greatly from the fabulous environment and colleagues in Cambridge (including George Batchelor, Herbert Huppert, Keith Moffatt, Tim Pedley, John Rallison, Grae Worster, John Sherwood, Oliver Harlen, Oliver Jensen and later John Lister to name just a few) who gave me more exposure to the breadth

of theoretical approaches to fluid mechanics problems than I had imagined possible. When I began at Harvard the mechanics group – Fred Abernathy, Bernie Budiansky, John Hutchinson, Richard Kronauer, Tom McMahon, Jim Rice and Lyle Sanders, along with two emeritus professors who represented the best of fluid mechanics, George Carrier and Howard Emmons – exposed me to many ideas in solid mechanics, material science and applied mathematics; I will always remember the formative years I spent with such a great group of colleagues and mentors. I have been very fortunate to have had many wonderful Harvard colleagues who have broadened my views and understanding, including Mike Aziz, Michael Brenner, David Nelson, Dave Weitz and George Whitesides. Of course, without my students and postdocs, none of this would have been possible. I have been lucky in this regard and I have long felt that I have the most wonderful research group, full of energy, ideas and initiative that has continually taught me new topics and exposed me to new ideas.

I thank my students Jacqueline Ashmore, John Bush (joint with Jeremy Bloxham), Magalie Faivre, Samuel Gaudet (joint with Gareth McKinley), Eric Lauga (joint with Michael Brenner), Michael Manga (joint with Rick O'Connell), Marcus Roper (joint with Michael Brenner), Kiril Selverov, John Tanzosh, Andre Valente (joint with David Edwards) and Wendy Zhang, and my postdocs Manouk Abkarian, Shelley Anna, Martin Bazant, Catherine Best, Laurent Courbin, Richard Day, Marc Durand, Cyprien Gay, Anthony Harkin, Sascha Hilgenfeldt, Stephan Koehler, Phil Lovalenti, Stephen Lucas, Sameer Madanshetty, Tom Powers, Bill Ristenpart, Amy Shen, Matt Sullivan, Thomas Ward and Dengfu Zhang. My current group of students – Anand Bala Subramaniam, Jacy Bird, Emilie Dressaire, Alison Forsyth, Renita Horton, Ann Lai, Rachel Pepper, Scott Tsai and Ernst van Nierop – and postdocs – Laura Guglielmini, Jinkee Lee, Sigolene Lecuyer, Mathilde Reyssat, Laurence Rongy, Roberto Rusconi, Benoit Scheid and Jiandi Wan – continue to inspire me with their creativity and hard work. I have also benefitted enormously from many opportunities to visit labs in France, and I recognize Armand Ajdari, Christophe Clanet, Laurent Limat, Jacques Magnaudet, David Quéré and Emmanuel Villermaux for hosting many such visits and for many inspiring questions and conversations over the years. Also, Jens Eggers has been a continual, very supportive and positive intellectual influence since my early years at Harvard. In recent years I have received generous financial support for my research from Unilever, Schlumberger, and Saint-Gobain, as well as from the Harvard MRSEC and NSEC centres sponsored by NSF; for all of this support I am very thankful. I thank John Brady for the remark about the drag on cylinder arrays as a further example of a two-dimensional viscous flow problem with a logarithmic correction. Jens Eggers, Emmanuel Villermaux and Grae Worster kindly provided helpful feedback on a draft of the paper. Finally, although I did not know George Batchelor well, I recognize and value the manifold contributions that he made to our field and this journal through his writings and leadership. Hopefully some of that impact is evident in the work described in this paper. Most of all, I recognize the value of family: from my parents who met after emmigrating to the United States from pre-World War II Germany, to my wife Valerie and our two children Taylor and Blaise. I dedicate this paper to them.

REFERENCES

Abkarian, M., Faivre, M. & Stone, H. A. 2006 High-speed microfluidic differential manometer for cellular-scale hydrodynamics. *Proc. Natl Acad. Sci. USA* **103**, 538–542.

Abkarian, M., Nunes, J. & Stone, H. A. 2004 Colloidal crystallization and banding in a cylindrical geometry. *J. Am. Chem. Soc.* **126**, 5978–5979.

Acrivos, A., Jeffrey, D. J. & Saville, D. A. 1990 Particle migration in suspensions by thermocapillary or electrophoretic motion. *J. Fluid Mech.* **212**, 95–110.

Ajdari, A. & Bocquet, L. 2006 Giant amplification of interfacially driven transport by hydrodynamic slip: diffusio-osmosis and beyond. *Phys. Rev. Lett.* **96**, 186102.

Anna, S. L., Bontoux, N. & Stone, H. A. 2003 Formation of dispersions using "flow focusing" in microchannels. *Appl. Phys. Lett.* **82**, 364–366.

Ashmore, J., Hosoi, A. E. & Stone, H. A. 2003 The effect of surface tension on rimming flows in a partially filled rotating cylinder. *J. Fluid Mech.* **479**, 65–98.

Aussillous, P. & Quéré, D. 2000 Quick deposition of a fluid on the wall of a tube. *Phys. Fluids* **12**, 2367–2371.

Batchelor, G. K. 1967 *An Introduction to Fluid Mechanics*. Cambridge University Press.

Batchelor, G. K. 1977 Developments in microhydrodynamics. In *Theoretical and Applied Mechanics: Proceedings of the 14th International Congress*, pp. 33–55. North-Holland.

Berg, H. & Turner, L. 1990 Chemotaxis of bacteria in glass capillary arrays – Escherichia coli, motility, microchannel plate, and light scattering. *Biophys. J.* **58**, 919–930.

Biesheuvel, A. & van Heijst, G. J. F. (Ed.) 1998 *In Fascination of Fluid Dynamics*. Springer.

Bretherton, F. P. 1961 The motion of long bubbles in tubes. *J. Fluid Mech.* **10**, 166–188.

Cheung, C., Hwang, Y. H., Choi, H. J. & Wu X.-L. 1996 Diffusion of particles in free-standing liquid films. *Phys. Rev. Lett.* **76**, 2531–2534.

Clément, E., Vanel, L., Rajchenbach, J. & Duran, J. 1996 Pattern formation in a vibrated granular layer. *Phys. Rev.* E **53**, 2972–2975.

Courbin, L., Denieul, E., Dressaire, E., Roper, M., Ajdari, A. & Stone, H. A. 2007 Imbibition by polygonal spreading on patterned surfaces. *Nat. Mater.* **6**, 661–664.

Courbin, L. & Stone, H. A. 2006 Impact, puncturing and the self-healing of soap films. *Phys. Fluids* **18**, 091105.

Crighton, D. G. 1981 Acoustics as a branch of fluid mechanics. *J. Fluid Mech.* **106**, 261–298.

Deegan, R. D., Bakajin, O., Dupont, T. F., Huber, G., Nagel, S. R. & Witten, T. A. 1997 Capillary flow as the cause of ring stains from dried liquid drops. *Nature* **389**, 827–829.

De Menech, M., Garstecki, P., Jousse, F. & Stone, H. A. 2007 Transition from squeezing to dripping in a microfluidic T-shaped junction. *J. Fluid Mech.* **595**, 141–162.

Derjaguin, B. 1943 Thickness of liquid layer adhering to walls of vessels on their emptying and the theory of photo- and motion-picture film coating. *C. R. (Dokl.) Acade. Sci. URSS* **39**, 13–16.

Durand, M. & Stone, H. A. 2006 Relaxation time of the topological T1 process in a two-dimensional foam. *Phys. Rev. Lett.* **97**, 226101-1-4.

van Dyke, M. 1982 *Album of Fluid Motion*. Parabolic Press.

Edwards, D. A., Brenner, H. & Wasan, D. T. 1991 *Interfacial Transport Processes and Rheology*. Butterworth-Heinemann.

Eggers, J. & Stone, H. A. 2004 Characteristic lengths at a moving contact line for a perfectly wetting fluid: the influence of speed on the dynamic contact angle. *J. Fluid Mech.* **505**, 309–321.

Faivre, M., Abkarian, M., Bikraj, K. & Stone, H. A. 2006 Geometrical focusing of cells in a microfluidic device: a route to separate blood plasma. *Biorheology* **43**, 147–159.

Fanton, X., Cazabat, A. M. & Quéré, D. 1996 Thickness and shape of films driven by a Marangoni flow. *Langmuir* **12**, 5875–5880.

Fuerstman, M. J., Lai, A., Thurlow, M. E., Shevkoplyas, S. S., Stone, H. A. & Whitesides, G. M. 2007 The pressure drop along rectangular microchannels containing bubbles. *Lab on a Chip* **7**, 1479–1489.

Garstecki, P., Fuerstman, M. J., Stone, H. A. & Whitesides, G. M. 2006 Formation of droplets and bubbles in a microfluidic T-junction – scaling and mechanism of breakup. *Lab on a Chip* **6**, 437–446.

de Gennes, P. G. 1985 Wetting: statics and dynamics. *Rev. Mod. Phys.* **57**, 857–863.

de Gennes, P. G., Brochard-Wyart, F. & Quéré, D. 2003 *Capillarity and Wetting Phenomena: Drops, Bubbles, Pearls, Waves*. Springer.

Gilet, T. & Bush, J. W. M. 2009 The fluid trampoline: droplets bouncing on a soap film. Chaotic bouncing of a droplet on a soap film. *J. Fluid Mech.* **625** 167–203.

Happel, J. & Brenner, H. 1983 *Low Reynolds Number Hydrodynamics*. Martinus Nijhoff.

Hinch, E. J. 1972 Note on the symmetries of certain material tensors for a particle in Stokes flow. *J. Fluid Mech.* **54**, 423–425.

Hosoi, A. E. & Bush, J. W. M. 2001 Evaporative instabilities in climbing films. *J. Fluid Mech.* **442**, 217–239.

Hunt, J. C. R. 1981 Some connections between fluid mechanics and the solving of industrial and environmental fluid-flow problems. *J. Fluid Mech.* **106**, 103–130. **76**, 2376–2378.

Jacobsen, K., Sheets, E. D. & Simson, R. 1995 Revisiting the fluid mosaic model of membranes. *Science* **268**, 1441–1442.

Kataoka, D. E. & Troian, S. M. 1999 Patterning liquid flow on the microscopic scale. *Nature* **402**, 794–797.

Koch, D. L. & Ladd, A. J. 1997 Moderate Reynolds number flows through periodic and random arrays of aligned cylinders. *J. Fluid Mech.* **349**, 31–66.

Koehler, S. A., Hilgenfeldt, S. & Stone, H. A. 1999 Liquid flow through aqueous foams: the node-dominated foam drainage equation. *Phys. Rev. Lett.* **82**, 4232–4235.

Koehler, S. A., Hilgenfeldt, S. & Stone, H. A. 2004 Foam drainage on the microscale. Part 1. Modelling flow through single Plateau borders. *J. Colloid Interface Sci.* **276**, 420–438.

Koehler, S. A., Hilgenfeldt, S., Weeks, E. R. & Stone, H. A. 2004 Foam drainage on the microscale. Part 2. Experiments on the scale of single Plateau borders. *J. Colloid Interface Sci.* **276**, 439–449.

Kuiken, H. K. (Ed.) 1996 *The Centenary of a Paper on Slow Viscous Flow by the Physicist H.A. Lorentz*. Kluwer Academic.

Landau, L. & Levich, B. 1942 Dragging of liquid by a plate. *Acta Physiochim. USSR* **17**, 42–54.

Lauga, E., Brenner, M. P. & Stone, H. A. 2007 Microfluidics: the no-slip boundary condition. In *Handbook of Experimental Fluid Mechanics* (ed. C. Tropea, A. Yarin & J. F. Foss), pp. 1219–1240. Springer.

Lauga, E., DiLuzio, W., Whitesides, G. M. & Stone, H. A. 2005 Swimming in circles: Motion of bacteria near solid boundaries. *Biophys. J.* **90** 400–412.

Leal, L. G. 1980 Particle motion in a viscous fluid. *Annu. Rev. Fluid Mech.* **12**, 435–476.

Leal, L. G. 2007 *Advanced Transport Phenomena: Laminar Flow and Convective Transport Processes*. Cambridge University Press.

Le Goff, A., Courbin, L., Stone, H. A. & Quéré, D. 2008 Energy absorption in a bamboo foam. *Europhys. Lett.* **84**, 36001-p1-p5.

Leonard, R. A. & Lemlich, R. 1965 A study of interstial liquid flow in foam. Part I. Theoretical model and application to foam fractionation. *AIChE J.* **11**, 18–24.

Levich, V. 1962 *Physicochemical Hydrodynamics*. Prentice Hall.

Lighthill, J. 1975 *Mathematical Biofluiddynamics*. SIAM.

Lorentz, H. A. 1896 A general theorem concerning the motion of a viscous fluid and few consequences derived from it. *Akad. Wet. Amsterdam* **5**, 168–175.

Manga, M. & Stone, H. A. 1993 Buoyancy-driven interactions between two deformable viscous drops. *J. Fluid Mech.* **256**, 647–683.

Mazouchi, A. & Homsy, G. M. 2000 Thermocapillary migration of long bubbles in cylindrical capillary tubes. *Phys. Fluids* **12**, 542–549.

Mysels, K. J., Shinoda, K. & Frankel, S. 1959 *Soap Films*. Pergamon Press.

Oron, A., Davis, S. H. & Bankoff, S. G. 1997 Long-scale evolution of thin liquid films. *Rev. Mod. Phys.* **69**, 931–980.

Pearson, J. R. A. 1981 Wider horizons for fluid mechanics. *J. Fluid Mech.* **106**, 229–244.

Peregrine, D. H. 1981 The fascination of fluid mechanics. *J. Fluid Mech.* **106**, 59–80.

Pomeau, Y. & Villermaux, E. 2006 Two hundred years of capillarity research. *Phys. Today* 39–44.

Pozrikidis, C. 1992 *Boundary Integral and Singularity Methods for Linearized Viscous Flow*. Cambridge University Press.

Probstein, R. F. 1994 *Physicochemical Hydrodynamics*. John Wiley & Sons.

Quéré, D. 1999 Fluid coating on a fibre. *Annu. Rev. Fluid Mech.* **31**, 347–384.

Ramachandran, A. & Khair, A. S. 2009 The dynamics and rheology of a dilute suspension of hydrodynamically Janus spheres in a linear flow. *J. Fluid Mech.* **633**, 233–269.

Ratulowski, J. & Chang, H. C. 1990 Marangoni effects of trace impurities on the motion of long gas bubbles in capillaries. *J. Fluid Mech.* **210**, 303–328.

Saffman, P. G. 1976 Brownian motion in thin sheets of viscous fluid. *J. Fluid Mech.* **73**, 593–602.

Saffman, P. G. & Delbrück, M. 1975 Brownian motion in biological membranes. *Proc. Natl Acad. Sci.* **72**, 3111–3113.

Samimy, M., Breuer, K. S., Leal, L. G. & Steen, P. H. (Ed.) 2004 *A Gallery of Fluid Motion.*Cambridge University Press.

Sangani, A. & Acrivos, A. 1982 Slow flow past periodic arrays of cylinders with applications to heat transfer. *Intl J. Multiph. Flow* **8**, 193–206.

Schleier-Smith, J. M. & Stone, H. A. 2001 Convection, heaping, and cracking in vertically vibrated granular slurries. *Phys. Rev. Lett.* **86**, 3016–3019.

Scriven, L. E. 1960 Dynamics of a fluid interface: equation of motion for Newtonian surface fluids. *Chem. Engng Sci.* **12**, 98–108.

Scriven, L. E. & Sternling, C. V. 1960 The Marangoni effects. *Nature* **187**, 186–188.

Sickert, M., Rondelez, F. & Stone, H. A. 2007 Single-particle Brownian dynamics for characterizing the rheology of fluid Langmuir monolayers. *Europhys. Lett.* **79**, 66005-1–6.

Singer, S. J. & Nicholson, G. L. 1972 The fluid mosaic model of the structure of cell membranes. *Science* **175**, 720–731.

Snoeijer, J. H., Ziegler, J., Andreotti, B., Fermigier, M. & Eggers, J. 2008 Thick films of viscous fluid coating a plate withdrawn from a liquid reservoir. *Phys. Rev. Lett.* **100**, 244502.

Squires, T. M. 2008 Electrokinetic flows over inhomogeneously slipping surfaces. *Phys. Fluids* **20**, 092105.

Stone, H. A. & Ajdari, A. 1998 Hydrodynamics of particles embedded in a flat surfactant layer overlying a subphase of finite depth. *J. Fluid Mech.* **369**, 151–173.

Tharmalingam, S. & Wilkinson, W. L. 1978 The coating of Newtonian liquids onto a roll rotating at low speeds. *Polym. Engng Sci.* **18**, 1155–1159.

Tirumkudulu, M. & Acrivos, A. 2001 Coating flows with a rotating horizontal cylinder: lubrication analysis, numerical computations and experimental measurements. *Phys. Fluids* **13**, 14–19.

Umbanhowar, P. B., Melo, F. & Swinney, H. L. 1996 Localized excitations in a vertically vibrated granular layer. *Nature* **382**, 793–796.

Wan, J., Ristenpart, W. D. & Stone, H. A. 2008 Dynamics of shear-induced ATP release from red blood cells. *Proc. Natl Acad. Sci.* **105**, 16432–16437.

Weaire, D. & Hutzler, S. 1999 *The Physics of Foams.* Oxford University Press.

Wilson, S. D. R. 1981 The drag-out problem in film coating theory. *J. Engng Math.* **16**, 209–221.

Wong, H., Radke, C. J. & Morris, S. 1995*a* The motion of long bubbles in polygonal capillaries. Part 1. Thin films. *J. Fluid Mech.* **292**, 71–94.

Wong, H., Radke, C. J. & Morris, S. 1995*b* The motion of long bubbles in polygonal capillaries. Part 2. Drag, fluid pressure and fluid flow. *J. Fluid Mech.* **292**, 95–110.

Young, N. O., Block, J. S. & Goldstein, M. J. 1959 The motion of bubbles in a vertical temperature gradient. *J. Fluid Mech.* **6**, 350–356.

Youngren, G. K. & Acrivos, A. 1975 Stokes flow past a particle of arbitrary shape: a numerical method of solution. *J. Fluid Mech.* **69**, 377–403.